Effect of High Pressure on the Photochemical Reaction Center from *Rhodobacter sphaeroides* R26.1

Andrew Gall,*† Aleksandr Ellervee,‡ Marie-Claire Bellissent-Funel,* Bruno Robert,† and Arvi Freiberg‡

*Laboratoire Léon Brillouin (CEA-CNRS) and †Section de Biophysique des Protéines et des Membranes, 91191 Gif-sur-Yvette, France; and ‡Institute of Physics, University of Tartu, Riia 142, EE51014, Estonia

ABSTRACT   High-pressure studies on the photochemical reaction center from the photosynthetic bacterium *Rhodobacter sphaeroides*, strain R26.1, shows that, up to 0.6 GPa, this carotenoid-less membrane protein does not loose its three-dimensional structure at room temperature. However, as evidenced by Fourier-transform preresonance Raman and electronic absorption spectra, between the atmospheric pressure and 0.2 GPa, the structure of the bacterial reaction center experiences a number of local reorganizations in the binding site of the primary electron donor. Above that value, the apparent compressibility of this membrane protein is inhomogeneous, being most noticeable in proximity to the bacteriopheophytin molecules. In this elevated pressure range, no more structural reorganization of the primary electron donor binding site can be observed. However, its electronic structure becomes dramatically perturbed, and the oscillator strength of its Q_y electronic transition drops by nearly one order of magnitude. This effect is likely due to very small, pressure-induced changes in its dimeric structure.

INTRODUCTION

In photosynthetic purple bacteria, the photosynthetic apparatus is rather simple, consisting of the photochemical reaction center (RC) and a network of interconnected light-harvesting (LH) proteins, all localized in intracytoplasmic membranes. In general, there are two types of LH proteins, LH1 and LH2. The noncovalently bound pigments in the LH antennae first absorb solar photons, and the resulting excitation energy is transferred to the RC where the transduction of excitation energy into chemical potential energy occurs (Van Grondelle, 1985). The x-ray crystal structures of a number of RCs have been determined with resolutions superior to 3.0 Å (Roy et al., 1995; Stowell et al., 1997; McAuley-Hecht et al., 1998; Fyfe et al., 1998). In *Rhodobacter* (*Rb.*) *sphaeroides*, it consists of three transmembrane-spanning polypeptides, two of which (L and M) possess very similar tertiary structures. Each of these polypeptides consists of five transmembrane-spanning helices that are linked by a series of small helices and loop regions. The H subunit is much less hydrophobic; it contains only a single membrane-protruding helix located at the N-terminal end of its sequence, and the rest of its structure is located at the membrane interface on the cytoplasmic side of the membrane. Altogether, the 10 helices of L and M form a cage inside of which are bound the RC cofactors. Each RC binds six bacteriochlorin pigments (four bacteriochlorophylls (Bchl) and two bacteriopheophytins (Bpheo)), two quinones, one carotenoid, and one non-heme iron. The

bacteriochlorin pigments and quinones are arranged in pairs around a pseudo-C_2 axis of symmetry that runs from the center of the primary donor of electrons (P, a pair of closely interacting Bchls) to the non-heme iron (Deisenhofer et al., 1984; Deisenhofer and Michel, 1989). Despite this apparent symmetry, electron transfer within the RC is highly asymmetric, occurring along the branch of cofactors most closely associated with the L subunit (the so-called L branch). Energy transduction is triggered by the excitation of P and results in unidirectional electron transfer from this Bchl dimer to the acceptor bacteriopheophytin (H_L), namely, $P \rightarrow B_L \rightarrow H_L$. This so-called primary charge separation initiates a series of electron transfers, which produce a chemical potential gradient across the membrane by oxidizing a c-type cytochrome at the periplasmic surface and reducing a quinone (Q_B) molecule on the cytoplasmic side of the membrane. A carotenoid molecule, which is noncovalently attached to the M-subunit, protects the protein from photo-oxidative damage (Frank and Cogdell, 1996; Cogdell and Frank, 1987). The *Rb. sphaeroides* strain R26.1 has lost the ability to synthesize carotenoids, and consequently its RC lacks this chromophore.

In bacterial RCs, the individual bacteriochlorins (Bchls and Bpheos), which are located throughout the volume of the protein, constitute a series of pigments that are able to monitor the localized structural changes when probed by electronic absorption and Raman spectroscopy. Their interactions with their immediate environments yield information on the structure of the photochemical RC and how the latter responds to external stress. In this sense, bacterial RCs constitute an ideal model for understanding the stability of membrane proteins. In turn, studying how these structural changes affect the electronic properties of these molecules may help in understanding the nature of the excited states involved.

In this paper, the Fourier transform (FT) Raman and absorption spectra of the RC from *Rb. sphaeroides* R 26.1 have been studied at high hydrostatic pressures. This combined approach has been proved fruitful for studying core light-harvesting (namely, LH1) proteins from purple bacteria (Sturgis et al., 1998). Indeed, resonance Raman spectroscopy, as a vibrational method, yields precise, detailed information on both the conformational (Näveke et al., 1997) and intermolecular interactions assumed by the bacteriochlorin cofactors present in photosynthetic proteins (Robert, 1996). With its help, the evolution of the localized changes at the pigment binding sites could be monitored as a function of applied hydrostatic pressure. The influence of pressure on the electronic levels of the different cofactors led to a description of which mechanisms were likely to play a role in tuning the electronic absorption of these proteins at atmospheric pressure and at physiological temperatures (Sturgis et al., 1998). Related works by Small and co-workers (Reddy et al., 1993, 1995, 1996; Small, 1995; Reddy and Small, 1996; Wu et al., 1996, 1997a,b, 1998, 2000; Pieper et al., 1999, 2000; Raetsep et al., 2000) on high-pressure hole-burning and absorption studies (both experimental and modeling) on photosynthetic membrane complexes have led to an evaluation of the electrostatic and electron-exchange interaction contributions toward the observed pressure shifts. Results of these studies suggest that charge-transfer state is an important contributor to pigment coupling and that any structural change may not be detectable by x-ray diffraction at current resolutions.

MATERIALS AND METHODS

Membrane preparation and protein isolation

Rb. sphaeroides R26.1 was cultured photosynthetically at 28°C in Böse medium (Böse, 1963); membranes were prepared and solubilized based on previously described methods (Feher, 1971; Clayton and Wang, 1971). Washed membranes were diluted to an A_{800} of 50 with Tris buffer (20 mM Tris-HCl, pH 8.0) and then solubilized with 0.35% *N,N*-dimethyldodecylamine-*N*-oxide (LDAO) for 90 min at 26°C followed by threefold dilution with Tris buffer. After high-speed centrifugation (250,000 × *g* for 70 min), the RC-containing supernatant was loaded onto a preequilibrated anion exchange column (20 mM Tris-HCl, pH 8.0, 0.1% LDAO, DEAE 650s, Fractogel, TosoHass, Montgomeryville, PA). After a salt gradient was applied (10–400 mM NaCl) the spectroscopically pure fractions were concentrated (Centriprep30, Amicon) and loaded onto a preequilibrated size exclusion column (0.075% LDAO, 50 mM NaCl, 10 mM Tris-HCl, pH 8.0, Fractogel TSK HW-55, TosoHass). Finally, the purified RCs were subjected to a second anion exchange column (Resource Q, Pharmacia). The polypeptide composition of the RCs was verified by polyacrylamide gel electrophoresis (Schägger and von Jagow, 1987); the gels were developed using the Silver Stain Plus kit (BioRad, Hercules, CA). For use in the high-pressure optical cell, samples were prepared in a buffer containing 0.05% LDAO, 10 mM Tris-HCl, pH 8.0 (Sigma, Milwaukee, WI).

High-pressure optical cell

The high-pressure optical cell used in this work has been shown to be able to reproducibly generate pressures up to a maximum of ~1 GPa and has

been described previously (Tars et al., 1994). Pressure was generated inside the cell by a hydraulic press and was transmitted to the sample by a liquid (glycerol-water) phase. Samples were allowed to equilibrate for 30 min after an increase in the pressure. Reversibility of the pressure-induced effects on the proteins was checked systematically by measuring absorption and/or FT Raman spectra upon pressure release after the pressure maximum had been applied.

Spectroscopy

RC samples were poised in their reduced (P) state using sodium ascorbate as previously described (Mattioli et al., 1991b). Room-temperature absorption spectra were recorded using a Cary 5 spectrophotometer (Varian, Sidney, Australia). For each applied pressure, at least two absorption spectra were recorded with a 30-min delay between measurements. These spectra were corrected by subtracting, at each applied pressure, a reference spectrum corresponding to that of the buffer alone in the pressure cell. Unless stated, the absorption spectra shown are from the second series of spectra, namely, 60 min after initial applied pressure (i.e., 30 min after the initial absorption spectrum). Before data analysis, the absorbance spectra were converted from nanometers to wavenumbers (cm^{-1}).

FT Raman spectra were recorded, using a Bruker IFS 66 interferometer coupled to a Bruker FRA 106 Raman module equipped with a continuous Nd:YAG laser, as described previously (Sturgis et al., 1998). Depending on sample conditions, spectra were the result of 4000–9000 co-added interferograms. This corresponded to between 100 and 225 min of data acquisition. To improve the precision of the data the Raman modes presented in Table 1 were obtained from second-derivative analysis. The reported frequencies are accurate to within ±1 cm^{-1}. The underlying background fluorescence was removed by fitting polynomial functions to the background signal, and second-derivative analyses were performed using GRAMS32 Spectral Notebase (Galactic Industries, Salem, NH).

RESULTS

Absorption spectra under pressure

Shown in Fig. 1 *a* is the effect of increasing pressure on the room-temperature near-IR absorption spectrum of the RC from *Rb. sphaeroides* strain R26.1. The absorption peaks at 760 and 802 nm arise from the Q_y absorption transitions of the Bpheo (H) and accessory Bchl (B) molecules, respectively. These pigments experience a quasi-linear pressure-induced red shift. As well as the pressure-induced red shift, the Q_y transition of the primary electron donor (P), located at 870 nm at atmospheric pressure, exhibits a decrease in intensity as a function of increasing pressure; this is emphasized in Fig. 1 *b* where the 0.05-GPa and 0.60-GPa applied pressures have been superimposed on the same *y* axis. When comparing these spectra, a slight decrease of the Q_x transition of the BChl molecules at ~600 nm as well as of the Q_y transition of the Bpheo molecules at 760 nm may be observed. This probably reflects a limited dilution (a few percent) of the sample in the transmission fluid during the time course of the experiment. None of these changes are a result of pigment loss from the protein as there is no increase of the intensity at ~770 nm, which is the expected absorption peak of the Q_y transition of free Bchl molecules. The reversibility of the pressure-induced effects on the RCs was checked systematically by measuring absorption spec-

TABLE 1 Evolution of selected Raman vibrational modes as a function of applied pressure

Mode/pressure (GPa)	Atm	0.02	0.10	0.15	0.20	Slope A (cm^{-1} GPa^{-1})	0.30	0.41	0.60	0.80	Slope B (cm^{-1} GPa^{-1})	Slope A + B (cm^{-1} GPa^{-1})
	204.6	205.6	206.2	207.0	207.6	13.5 ± 1.1	207.4	208.5	209.7	210.8	6.6 ± 0.9	7.0 ± 1.8
	335.0	335.3	336.8	336.9	336.6	9.2 ± 0.9	337.5	338.8	340.1	340.9	6.6 ± 0.9	7.3 ± 1.9
Sapphire cell windows		417.7	417.9	417.9	417.9	0.6 ± 0.1	418.0	418.1	418.6	418.9	1.9 ± 0.3	1.4 ± 0.4
Ring V	565.5	565.5	566.2	566.4	566.9	7.1 ± 0.7	567.4	567.8	568.3	569.0	3.1 ± 0.5	4.3 ± 1.2
δCCC	584.6	584.8	584.8	584.6	584.8	0.3 ± 0.1	584.7	584.8	584.8	585.3	1.1 ± 0.2	0.6 ± 0.2
	650.3	651.3	652.0	652.3	561.8	8.0 ± 0.7	651.8	651.8	652.0	652.8	1.9 ± 0.4	2.1 ± 0.7
	683.1	683.4	683.1	683.6	683.8	2.8 ± 0.4	684.4	684.8	685.3	686.0	3.1 ± 0.5	3.7 ± 1.0
δCNC	727.6	728.0	728.1	728.3	729.0	5.6 ± 0.6	729.4	729.5	729.8	730.3	1.8 ± 0.8	3.0 ± 0.9
	788.0	788.2	789.1	789.2	789.2	6.5 ± 0.5	789.0	789.7	790.0	789.8	1.4 ± 0.1	1.8 ± 0.6
	893.6	894.3	895.3	895.5	895.5	9.3 ± 1.0	896.6	897.1	898.1	899.2	5.2 ± 0.9	6.0 ± 1.7
	923.3	923.3	923.5	923.7	923.8	2.7 ± 0.4	924.4	925.2	926.0	926.3	3.7 ± 0.5	4.3 ± 1.1
R$_6$ νCaN(II,IV), νCaCb(I,II)	1012.7	1012.7	1013.3	1013.7	1014.7	9.5 ± 0.9	1014.8	1015.4	1016.6	1016.9	4.4 ± 0.6	5.5 ± 1.5
	1114.6	1115.0	1115.2	1115.2	1115.2	2.5 ± 0.2	1115.3	1116.1	1117.7	1118.3	6.2 ± 0.9	4.6 ± 1.2
R$_5$ νCaN(IV), νCaCb(II), δCbCaN(III), δCmH(α,β)	1135.4	1135.4	1136.4	1136.7	1136.7	7.5 ± 0.7	1137.4	1138.3	1138.9	1139.7	4.3 ± 0.6	5.4 ± 1.4
R$_4$	1159/1170	?	?	?	?	?	?	?	?	?	?	?
	1249.9	1250.0	1250.5	1250.3	1250.0	1.0 ± 0.2	1250.1	1251.1	1252.6	1253.9	7.6 ± 1.1	4.8 ± 1.3
	1258.8	1258.8	1259.7	1258.8	1259.9	4.2 ± 0.6	1260.3	1261.6	1261.8	1264.1	6.8 ± 1.1	6.4 ± 1.7
	1327.2	1329.1	1329.1	1329.1	1329.3	7.0 ± 0.7	1329.3	1330.0	1333.0	1333.1	8.4 ± 1.4	6.6 ± 1.8
	1355.7	1356.1	1357.1	1357.8	1357.1	8.5 ± 0.8	1357.9	1357.9	1358.0	1358.0	0.2 ± 0.0	2.4 ± 0.8
	1368.4	1368.6	1368.6	1368.9	1369.2	3.5 ± 0.4	1369.5	1369.5	1369.7	1370.6	2.2 ± 0.5	2.5 ± 0.7
	1373.3	1373.3	1373.3	1373.3	1373.3	0.0 ± 0.0	1373.3	1373.5	1374.1	1374.2	1.6 ± 0.3	0.9 ± 0.3
	1439.3	1439.4	1441.0	1441.2	1440.4	7.9 ± 0.7	1440.8	1441.3	1443.1	1444.6	7.9 ± 1.3	5.9 ± 1.6
R$_3$ νCaN, νCaCm	1528.3	1528.7	1529.5	1530.5	1531.0	13.5 ± 1.3	1532.0	1532.1	1533.8	1534.1	4.8 ± 0.9	7.4 ± 2.0
R$_2$	1539.6	1539.9	1540.7	1541.2	1542.2	12.2 ± 1.4	1543.7	1544.7	1547.2	1548.5	10.0 ± 1.6	11.7 ± 3.0
	1584.5	1584.5	1584.5	1584.2	1585.1	1.2 ± 0.5	1585.7	1585.1	1587.5	1587.8	5.3 ± 1.2	4.6 ± 1.3
R$_1$ νCaCm(α,β,γ,δ)	1607.0	1607.0	1608.6	1610.4	1611.7	24.3 ± 2.2	1612.5*	1613.2*	1614.0*	1615.6*	6.0 ± 1.0	10.6 ± 2.9
P$_L$ ν2C=O	1619.8	1621.0	1619.3	1619.6	1615.1	20.9 ± 1.6	?	?	?	?	?	?
P$_M$ ν2C=O	1652.3	1652.4	1652.0	1651.7	1651.6	−4.1 ± 0.4	1651.3	1650.0	1650.0	1648.3	−5.2 ± 0.8	−4.9 ± 1.3
P$_M$ ν9C=O	1679.0	1678.7	1679.0	1679.0	1678.9	0.4 ± 0.6	1680.6	1680.9	?	?	2.7 ± 0.0	5.8 ± 0.8
P$_L$ ν9C=O	1692.6	1692.6	1692.7	1693.0	1693.0	2.3 ± 0.2	1692.9	1693.1	?	?	1.8 ± 0.0	1.2 ± 0.2

The modes marked with an asterisk (*) are a result of converging Raman lines (see text). Raman mode assignments are in Fisher nomenclature (Fisher and Orth, 1937; Fisher and Stern, 1940). Excitation wavelength λ_{ext} = 1064 nm; experimental temperature T = 293 K.

tra upon pressure release, after the pressure maximum had been applied, and found to be fully elastic for the cycle of pressure investigated (1 atm-0.6 GPa). This is in agreement with the previous work (Freiberg et al., 1993; Tars et al., 1994; Sturgis et al., 1998).

The variations of the energies of the different Q_y transitions according to pressure are displayed in Fig. 2. For the pressure cycle investigated (0.05–0.6 GPa), the Q_y transition of the Bpheo molecules (Fig. 2; H) shows a quasi-linear relationship with applied pressure with a slope of -294 ± 6 cm^{-1} GPa^{-1}. Similar slopes are observed for the accessory Bchl Q_y transition (-305 ± 13 cm^{-1} GPa^{-1}) for the pressures less than, or equal to, 0.4 Gpa (Fig. 2; B). However, for applied pressures greater than 0.4 GPa the pressure sensitivity characterized by the slope reduces by $\sim 1/3$, down to -118 ± 1 cm^{-1} GPa^{-1}. This change in slope cannot be due to an error in data acquisition. An analysis carried out on different series of absorption spectra for the same pressure range yielded comparable results (not shown).

The Q_y transition of the primary electron donor dimer exhibits a more complex behavior as a function of pressure than the transitions of the monomeric bacteriochlorins bound to the RC (Fig. 2; P). Between 0.05 and ~ 0.2 GPa an apparent quasi-linear red shift occurs with a slope of -528 ± 38 cm^{-1} GPa^{-1}. Then the energy of the transition remains almost unchanged with the pressure up to ~ 0.3 GPa. Upon a further increase of the pressure one may observe yet another, but different, apparent quasi-linear pressure-induced red shift with a steeper slope of -670 ± 28 cm^{-1} GPa^{-1}.

Shown in Fig. 3 a are the Q_x absorption bands of the Bchl (~ 600 nm) and the Bpheo (~ 535 nm) molecules at the minimal applied pressure (0.05 GPa) and at 0.6 GPa. Unlike the Q_y transitions of Bchls (B and P), in the Q_x region all the different Bchl molecules contribute to a single absorption band at room temperature. Despite that, the behavior of the Q_x band under pressure is very similar to that of the Q_y band. For the pressures ≤0.4 GPa a pseudo-linear downshift of the Bchl Q_x transition energy with the rate of -307 ± 9
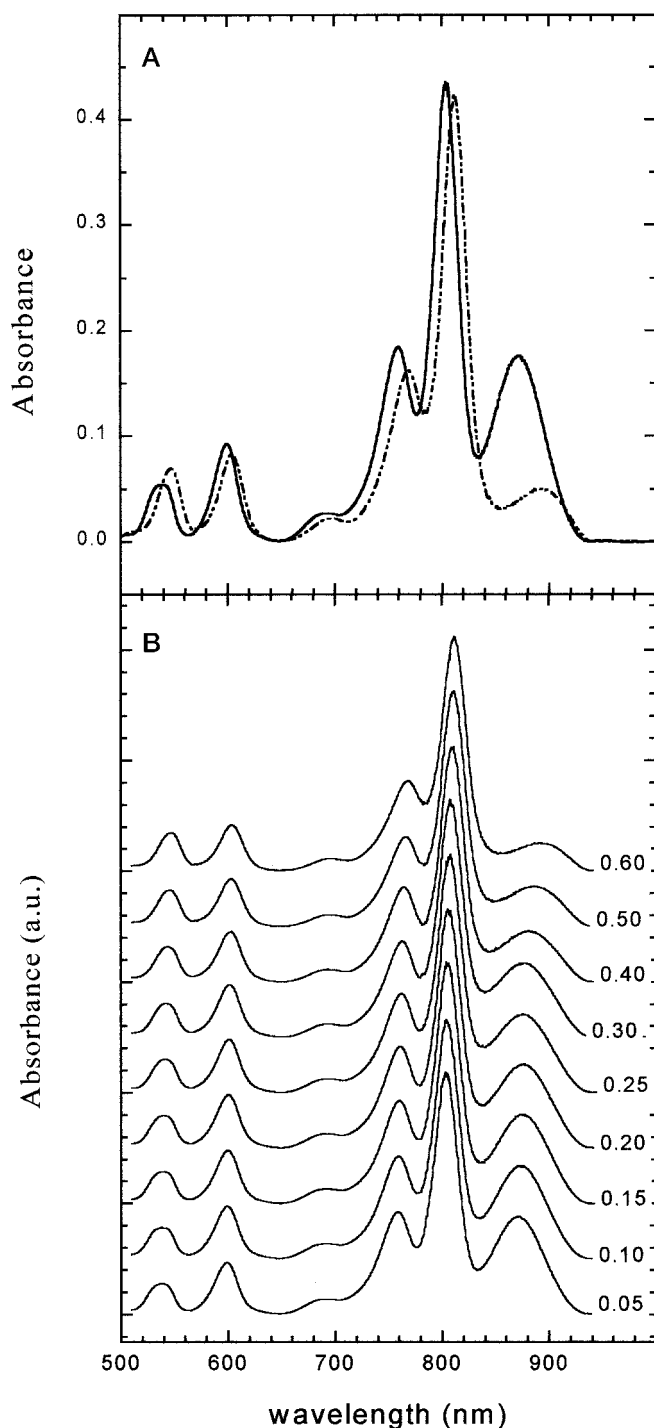
FIGURE 1   The effect of pressure on the electronic absorption spectrum of isolated RC from *Rb. sphaeroides* R26.1 measured at room temperature. (*a*) The numbers at each curve indicate the pressure in GPa at which the different spectra were recorded; (*b*) To clearly illustrate the general red-shift of all the Q_x and Q_y electronic transitions as well as the reduction in P at 0.6 GPa the spectra at 0.05 GPa (*solid line*) and 0.6 GPa (*broken line*) have been superimposed on the same axes.
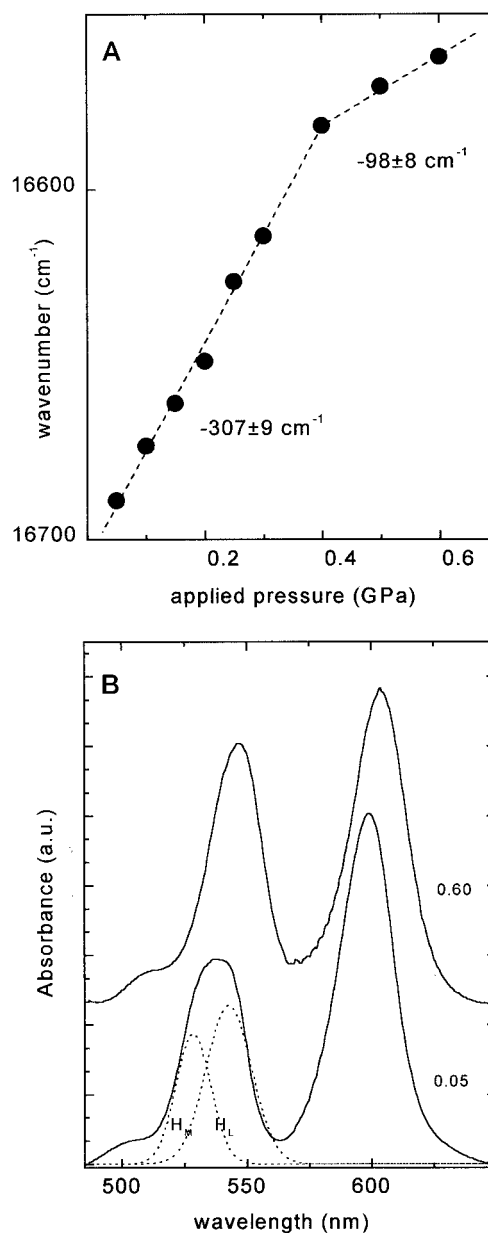

FIGURE 2   The effect of pressure on the Q_x absorption transitions of the Bpheo and Bchl molecules in isolated reaction centers measured at room temperature. (*a*) Absorption spectra at 0.05 GPa (*bottom trace*) and 0.6 GPa (*top trace*). The contributions of the two Bpheo molecules, H_L and H_M, are estimated (*dotted trace*; see text). (*b*) Pressure sensitivity of the Q_x transition frequency of Bchl.

cm^{-1} GPa^{-1} is observed (Fig. 3 *b*). At higher applied pressures, the pressure sensitivity reduces by $\sim 1/3$ to -98 ± 8 cm^{-1} GPa^{-1}. As for the Bpheo band, it is known that at atmospheric pressure the Q_x bands of H_M and H_L have slightly different absorption maxima, which results in a flattened absorption peak (Fig. 3 *a*, lower trace) (Parson and Cogdell, 1975). Applying Gaussian distributions to the Q_x bands of Bpheo measured at 0.05 GPa, we obtained the
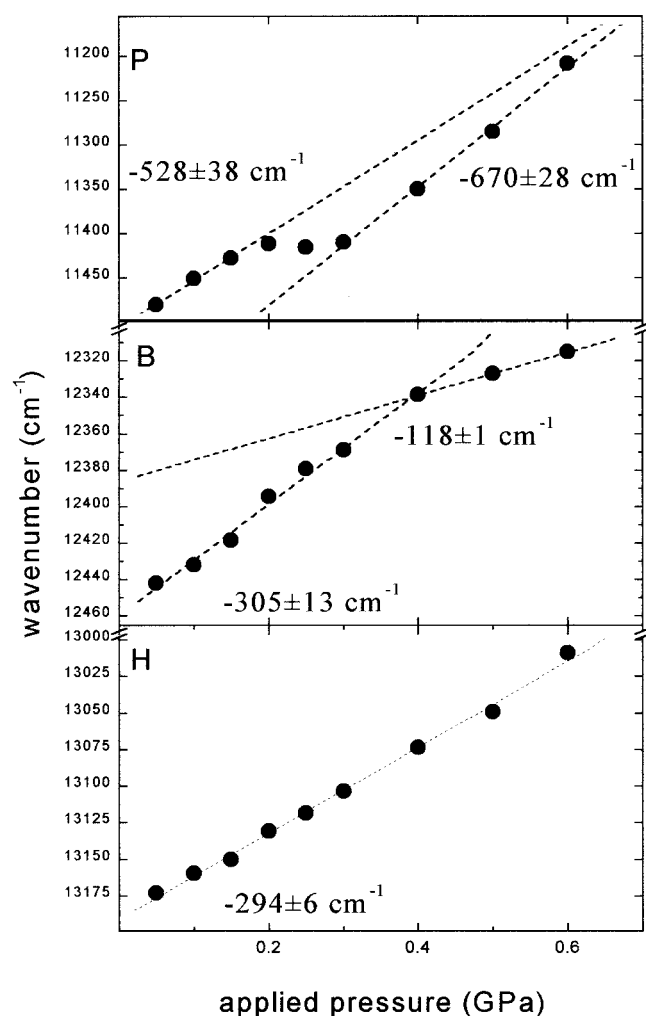
FIGURE 3   Pressure sensitivity of the Q_y transition frequency of H, B, and P in isolated RCs, measured at room temperature.

electronic transitions ascribed to H_M and H_L proved near impossible due to their spectral convergence.

The total integrated area for all the absorption bands is calculated and normalized to the spectrum at the atmospheric pressures (0.0001 GPa) (see Fig. 4). It appears that the area under the Q_x absorption bands as well as the Q_y bands of the Bpheo and accessory Bchl molecules does not reduce when external pressure is applied. By contrast, a dramatic drop of the intensity of the Q_y transition of the primary electron donor is observed for pressures higher than 0.3 GPa. Interestingly, not only the integrated areas but also the widths (not shown) of all the electronic transitions, except P, were found to be practically invariant with pressure. The loss of intensity in the P band is expected to be compensated by the appearance of extra intensity somewhere in the absorption spectra. It is, however, difficult to determine precisely what occurs in the Soret region between spectra taken at different pressures. In the blue region of the spectra, the baseline appears to be very sensitive to pressure. Although, as mentioned above, the spectra were corrected by baselines constituted by absorption spectra of the buffer in the pressure cell at each pressure, this correction is not accurate enough to precisely evaluate whether the changes observed in this spectral region compensate the loss in the Q_y transitions. It must be underlined that a 0.5% drift of the baseline is enough to induce a spectral change in the 350–400-nm region of similar intensity of that observed at 850 nm upon pressure application.

Comparing the evolution of spectra with time at a given pressure may help in determining precisely what occurs in the different spectral areas upon the decrease in intensity of the Q_y transition of P. Therefore, to further characterize the observed pressure sensitivity of the P absorption band intensity, the absorption spectra at 0.3 and 0.6 GPa were
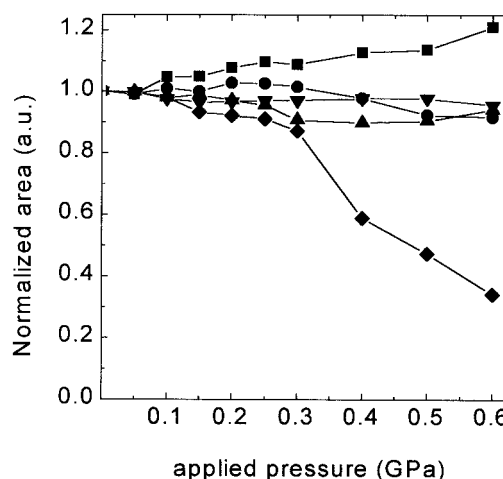
dotted curves in Fig. 3 *a* that approximate the electronic absorption bands of H_M and H_L with absorption maxima at ~530 and 543 nm, respectively. This analysis is in fair agreement with previous results (Parson and Cogdell, 1975) carried out at atmospheric pressure. At 0.6 GPa these two peaks appear to converge giving a single absorption maximum at 547.8 nm. The Q_x band of H_L thus experiences an ~4.6 nm (~262 cm^{-1}) red shift, whereas that of H_M appears to be more sensitive to applied pressure and must experience a red shift greater than 12 nm (~614 cm^{-1}). This remarkably different pressure sensitivity of the Q_x electronic transition energies of the two Bpheo molecules underscores the inherent inhomogeneity of the RC protein interior around the C_2 symmetry axis. The merger of the two Bpheo bands also accounts for the apparent pressure-associated increase in peak intensity of the Bpheo band relative to the Q_x absorption band of the Bchls. The calculations of the shift rate as a function of applied pressure for the Q_x

FIGURE 4   Integrated areas for the Q_y transitions of H (▲), B (▼), and P (♦) in isolated RCs and for the Q_x transitions of Bpheo (■) and Bchl (●) molecules, measured at room temperature. The spectra were normalized against the spectrum obtained at atmospheric pressure (see text).

measured as a function of time. Shown in Fig. 5 are the Q_y absorption band of P and the reference Q_x absorption band of all Bchls for both pressures. As seen, at each pressure the position of the reference Bchl-Q_x transition remains virtually constant as a function of time. Moreover, the integrated areas are near identical, indicating that no temporal loss of signal is present. The temporal intensity loss of the Q_y absorption band of P is also negligible for pressures less than 0.3 GPa. At 0.3 GPa very little loss of intensity is observed during the first 90 min. After 900 min, the integrated area of this absorption band is reduced by 20%. At 0.6 GPa, a similar reduction (23%) in intensity is observed already within the first 90 min. Furthermore, at 0.6 GPa the rate of drift in the baseline appears to be reasonably constant with time allowing the entire spectral region, from 350 to 1000 nm, to be precisely evaluated as absorption intensity over wavenumber. These difference plots were obtained from untreated spectra, namely, without any baseline subtraction (e.g., Fig. 6 *a*; 0 min (solid line) and 90 min (dotted line)). To demonstrate this, Fig. 6 shows the difference spectrum (in wavenumbers) between 0 and 90 min (Fig. 6 *b*, solid line) and the corresponding spectrum for the next temporal increment, namely, the difference between 30 and 120 mins (Fig. 6 *b*, dotted line). Therefore, allowing for the slight temporal drift of the baseline, especially in the sensitive blue region of the spectra, it appears that the loss of intensity in the Q_y transition in P is nearly exactly compensated by additional intensity in the Soret transition.

Preresonant FT Raman spectra under pressure

To investigate more closely the molecular mechanisms underlying the pressure sensitivity of the Bchl absorption
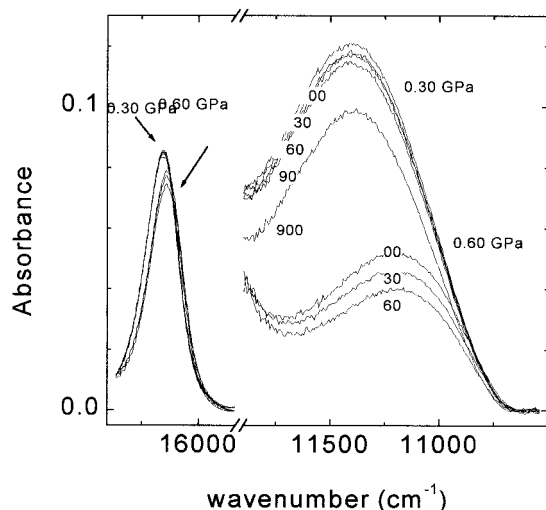

FIGURE 6   Difference spectra (in wavenumbers) between 0 min and 90 min (*solid line*) and the between 30 and 120 min (*dotted line*) obtained from absorption spectra without any baseline subtraction. Allowing for the slight temporal drift of the baseline (see text), it appears that the loss of intensity in the Q_y transition in P is nearly exactly compensated by additional intensity in the Soret transition.

properties, FT Raman spectra of the RC protein at various applied pressures were measured. As was already mentioned, this vibrational technique provides information both on the conformation of the chromophores and on the intermolecular interactions in which these chromophores are involved (Näveke et al., 1997; Robert, 1996). When using an excitation wavelength of 1064 nm, FT Raman spectra of RCs from purple bacteria contain contributions mainly from the two Bchls of the primary electron donor (Mattioli et al., 1991b). Thus, FT Raman spectra recorded under these conditions produce highly selective information on the conformation of, and intermolecular interactions assumed by, these specific bacteriochlorin molecules. (Mattioli et al., 1991a, 1993, 1994).

FT Raman spectra of isolated RCs from *Rb. sphaeroides* R26.1 were recorded at eight different pressures: atmospheric pressure (0.0001 GPa) and 0.10, 0.15, 0.20, 0.30, 0.40, 0.60, and 0.80 GPa. In Fig. 7 we show the 200-cm^{-1} to 1800-cm^{-1} region of the FT Raman spectra obtained at 0.02 GPa, (middle trace) and 0.80 GPa (upper trace). These spectra of Fig. 6 are normalized on the P contributions. The lower trace in Fig. 7 shows the FT Raman spectrum of a sapphire window of our high-pressure cell, characterized with three modes at 379, 417, and 645 cm^{-1}. Therefore, the sample spectra under pressure also contain these signatures. An asterisk in all three traces of Fig. 7 marks the main sapphire band at ~417 cm^{-1}. This band, which has a pressure sensitivity of 1.4 cm^{-1} GPa^{-1} (see Table 1), was

FIGURE 5   Temporal evolution of P and Q_x-Bchl absorption bands at 0.3 and 0.6 GPa. The numbers indicate the time in minutes at which the different spectra were recorded after an initial delay of 30 min after a change in pressure. One may note that, discounting the previously discussed red shift, the Q_x spectra at each pressure are invariant.
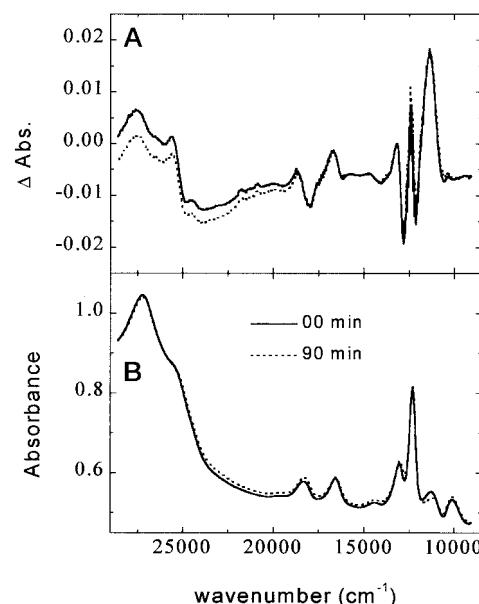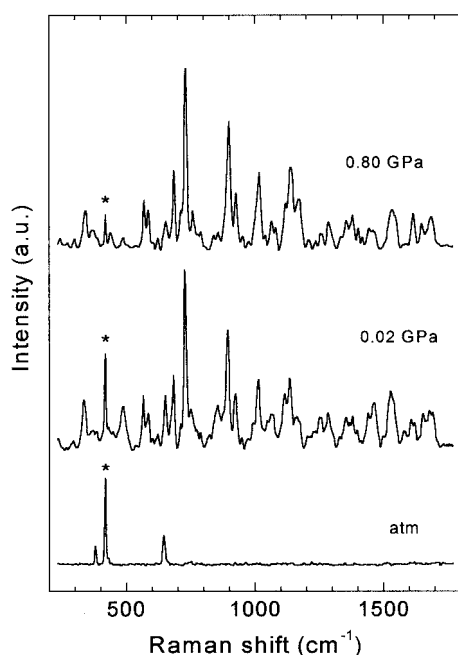
FIGURE 7 The effect of pressure on the 200-1800-cm^{-1} region of the room temperature FT Raman spectrum of the bacteriochlorin molecules in the RC complex. Upper trace, 0.8 GPa; middle trace, 0.2 GPa; lower trace, empty high pressure cell, atmospheric pressure. Excitation wavelength λ_{ext} = 1064 nm.

used as an internal scattering intensity standard. It appears that, although the oscillator strength of the Q_y transition of P decreases by nearly an order of magnitude between atmospheric pressure and 0.8 GPa (not shown), the pressure boost results in an increase in the resonance enhancement of the P contributions into the FT Raman spectrum. This effect, which is a result of the increasing overlap of the P absorption spectrum with the spectrum of the exciting laser light, may be observed in Fig. 7. In the spectrum recorded at 0.8 GPa, the intensity of the 417-cm^{-1} band is nearly three times smaller than in the spectrum recorded at atmospheric pressure.

Table 1 displays the major frequencies observed in the FT Raman spectra from the RC protein for each applied pressure. As the absorption spectrum of P indicates that a major change in pressure sensitivity occurs between 0.2 and 0.3 GPa, the slopes were calculated for the lower (0.001–0.2 GPa,) and upper (0.3–0.8 GPa) applied pressure ranges and are designated slope A and B, respectively. The last column (slope A + B) indicates the pressure sensitivity of each observed mode assuming no such partitioning of the data exists. The observed upshifts (0–5 cm^{-1} GPa^{-1}) of the vibrational frequencies upon employment of hydrostatic pressure are typical for organic molecules (Zhou et al., 1996). Similar Raman shifts have recently been reported in the LH1 complex from *Rhodospirillum* (*Rsp.*) *rubrum* for a similar pressure range (Sturgis et al., 1998). They may be explained taking into consideration both the effect of pres-

sure on the harmonic force constant and the anharmonicity of the oscillator (Benson and Dricamer, 1957; Zhou et al., 1996). When the effect of pressure on the harmonic force constant is dominant, upshifts of the vibrational frequency under pressure reflects a strengthening of the intramolecular bonds whereas frequency downshifts reflect bond weakening. Because the observed frequency shifts observed in the RC are small, less than ~1% of the frequency of the relevant modes, the pressure-induced force constant changes are probably sufficient to explain them.

In a recent FT Raman study, Näveke et al. (1997) have shown that the frequencies of six Bchl modes (named R_1–R_6) were sensitive to the distortions of the Bchl macrocycle. For the penta-coordinated Bchl in diethyl ether, the R_{1-6} frequencies are observed at 1609, 1536, 1445, 1158, 1140, and 1017 cm^{-1}, respectively (Näveke et al., 1997). More recently, the same modes have been identified in bacterial RCs at 1606, 1530/1537, 1439, 1159/1170, 1140, and 1013 cm^{-1} (Lapouge et al., 1999). At the minimal applied pressure the modes R_{1-3}, R_5, and R_6 are at ~1607, 1540, 1528, 1135, and 1013 cm^{-1} (see Table 1), and they all exhibit a rather high pressure sensitivity (greater than ~8 cm^{-1} GPa^{-1} in the 0.0001–0.2 GPa range). Under pressure the R_4 band is masked by other Raman modes. It is known that the frequencies of the R_4 and R_5 modes located in Table 1 at 1439 and 1135 cm^{-1}, respectively, are not sensitive to changes in the dielectric properties of the Bchl environment (Lapouge et al., 1998). In FT Raman spectra of LH1 antenna proteins, the frequencies of these modes were also not particularly sensitive to the pressure (Sturgis et al., 1998). It must thus be concluded that, in bacterial RCs, the large frequency upshifts upon applying pressure reflects a change in the conformation of the Bchl molecules constituting the primary electron donor, those becoming more distorted when external hydrostatic pressure is applied.

At first approximation, the frequencies of the R_{1-6} modes may be considered as linearly dependent on the core size of the Bchl molecules. In the frame of this approximation, the variations observed upon increasing the pressure from atmospheric pressure to 0.2 GPa correspond to a reduction of the core size of the Bchl constituting P between 0.007 and 0.009 Å (Näveke et al., 1997). To give an estimate of the extent of this conformational change, it may be said that this reduction of the molecular core size corresponds to a macrocycle distortion, of approximately half of what is observed between Bchl molecules having their central Mg atom 6- and 5-coordinated. Of course, as already discussed in Lapouge et al. (1999), the frequency shifts observed must correspond to changes in the angles between the pyrrole rings and the tetrapyrrole plane, and such a description of the Bchl conformational change in terms of molecular core size is only approximate.

Fig. 8 displays the high-frequency region of the FT Raman spectra of R26.1 RCs as a function of applied hydrostatic pressure. In this region, at atmospheric pressure, four
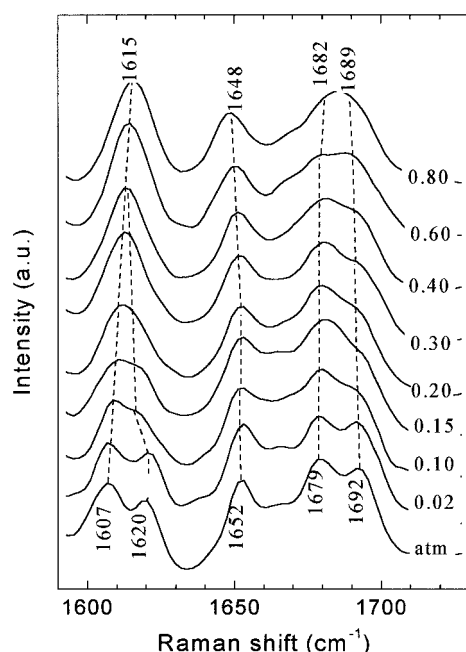
FIGURE 8 The effect of pressure on the high-frequency region (1575–1750 cm^{-1}) of the room temperature FT Raman spectrum of bacterio-chlorin molecules in the RC complex. The numbers at each curve indicate the pressure in GPa at which the different spectra were recorded. Excitation wavelength λ_{ext} = 1064 nm.

stretching modes other than the R$_1$ mode at 1607 cm^{-1}, have been identified (Mattioli et al., 1991b, 1993, 1994; Wachtveitl et al., 1993). The two bands at 1620 and 1652 cm^{-1} arise from the stretching modes of the acetyl carbonyl groups of P$_L$ and P$_M$, respectively. The last two Raman bands at 1679 and 1692 cm^{-1} are due to the stretching modes of the keto carbonyl groups of P$_M$ and P$_L$, respectively. (The R$_1$ mode arises from the stretching modes of the methine bridges (νCaCm($\alpha,\beta,\gamma,\delta$)) of both P$_L$ and P$_M$.) These vibrational modes have been extensively studied both in vitro and in vivo, and it is well established that their frequencies primarily depend on the strength of the inter-molecular interactions that the carbonyl groups are involved in. Of the four carbonyls belonging to the primary donor only the acetyl group of P$_L$ interacts with a neighboring residue, namely, the N$_\delta$H of the histidine residue L168 (His$_{L168}$) (Mattioli et al., 1994; Michel and Deisenhofer, 1988). Upon applying external pressure, the frequencies of three of four bands in Fig. 8 remain relatively unchanged. However, upon close examination of Fig. 8 the 1620-cm^{-1} mode rapidly downshifts to 1615 cm^{-1} for the pressure range between 0.02 and 0.2 GPa. This behavior, which is observed for this mode only, reflects an increase in the intermolecular interaction between the acetyl of P$_L$ and its histidine partner. At elevated pressures, a partial loss of the resolution between bands is observed, reflecting a gradual broadening of every band present in this spectral range.

At higher pressures (0.2–0.8 GPa), the Raman bands reflecting the macrocycle conformation are less sensitive to the pressure (see Table 1). Also, no further spectral change is observed in the carbonyl region. This is a good indication that the overall structure of the bacterial RC is stable at room temperature even when the pressure reaches 0.8 GPa. Unfolding of the protein would result in more dramatic changes in the Raman spectrum (Mozhaev et al., 1996). The same conclusion was drawn for the LH1 antenna from the related bacterium *Rsp. rubrum* (Sturgis et al., 1998). Although the structure of the bacterial RC does not unfold, FT Raman spectra obtained at the highest pressures become less well defined, indicating an increase in the inhomogeneous broadening of the bands arising from the different carbonyl stretching modes. This suggests that the RC structure becomes more disordered at these very high hydrostatic pressures. Additional experiments are clearly needed in the 0.8–1.2-GPa range to determine whether we have reached the limit for the photosynthetic membrane protein stability.

DISCUSSION

High-pressure studies on the bacterial reaction centers show that, up to 0.8 GPa, this protein does not lose its three-dimensional structure. However, between the atmospheric pressure and ~0.2 GPa, the structure of bacterial RCs experiences a number of local reorganizations in the macrocycles of the two Bchl molecules of the primary electron. In the same pressure range, a strengthening of the H-bond between the acetyl carbonyl of P$_L$ and the neighboring N$_\delta$H of the imidazole ring of His$_{L168}$ is observed, most probably indicating a shortening of its length. Taken together, these results indicate that, in this pressure range, the protein binding site of P experiences a significant reorganization. It should be noted that decreasing the temperature from 293 to 10 K induces similar effects on the FT Raman spectra to those observed when increasing pressure from 0.0001 to 0.2 GPa (Ivancich et al., 1997). At 10 K, a distortion of the P molecules was observed, as well as a strengthening of the H bond between His$_{L168}$ and the acetyl carbonyl of P$_L$. The possibility of a contraction of the RC structure when lowering temperature was evoked by Ivancich et al. (1997) to explain the observed changes in the FT Raman spectra. The present results support this hypothesis.

Pressure-induced energy shifts of the electronic transitions from organic molecules have been studied in a number of cases. For a small molecule dissolved in solid media, they depend on the following expression:

$$\Delta\nu(P) = 2\kappa\nu_s\Delta P, \qquad (1)$$

where $\kappa = -(1/V)(dV/dP)$ is the isothermal compressibility of the medium surrounding the absorbing molecule and ν_s represents the solvent shift of the solute electronic transition (i.e., the shift between the molecule in the solvent and the

gas phase (Sesselmann et al., 1987; Laird and Skinner, 1989)). Of course, this expression does not apply for strongly (excitonically) coupled solute molecules. In the latter case, due to modification by external pressure the relative distances between, and/or geometry of, the coupled molecules, the coupling energy and, thus, the absorption properties of the molecular aggregate will change. In the case of molecules embedded into proteins, it is also clear that some of the assumptions used to receive Eq. 1 do not apply. In particular, deriving Eq. 1 requires that the elastic properties of the matrix are isotropic and homogeneous, which is certainly not the case in proteins. Despite these obstacles, Eq. 1 proved to yield useful qualitative information on the local compressibilities of the proteins when probed by chromophores, which are only weakly coupled to the other pigment molecules in the protein (Tars et al., 1994).

This work has shown that above 0.2 GPa, the apparent compressibility is inhomogeneous, being most noticeable in proximity to the Bpheo molecules in that the Q_x transition of the accessory Bpheo, H_M, experiences a larger shift upon external pressure than that of the H_L acceptor Bpheo. The local compressibility of the RC should thus be higher in the H_M protein-binding site. Our results are in good agreement with the crystallographic data (protein database accession code 4RCR (Feher et al., 1989)) associated with each of these molecules, indicating that H_M is less structurally defined at room pressure than H_L, particularly along its x axis (Yeates et al., 1988).

As shown in Fig. 3, up to ~0.4 GPa, the Q_y absorption bands of the accessory Bchl and Bpheo molecules have very similar absorption band displacements. Moreover, their behavior is quite similar to that observed for the isolated Bchl and porphyrin molecules in solutions at room temperature (Tars et al., 1998). Although structural reorganizations of these pigments cannot be formally excluded, it is more likely that the observed shift arises purely from the compressibility of the surrounding RC protein structure. At pressures greater than 0.4 GPa, there is a drastic decrease in the pressure sensitivity of the accessory Bchl electronic transition energies. Although other mechanisms may be involved, this more than likely indicates a decrease of the local compressibility of the RC. Presumably this would affect transient absorption measurements under pressure. Previous works by Windsor and co-workers on the effect of pressure on charge recombination step in reduced RCs from *Rb. sphaeroides* R26 have suggested that increasing the pressure increases the rate of the charge recombination step $p^+H_L^-Q_A^- \rightarrow PH_LQ_A^-$ and that it may be sensitive to the distance between P and Q_A (Windsor and Menzel, 1989; Hoganson et al., 1987). This trend was reversed at 0.35 GPa (Redline et al., 1991). It is worth noting that 0.4 GPa corresponds to a value at which many soluble globular proteins unfold, i.e., at which further decrease in volume requires the loss of their folded structure (Mozhaev et al.,

1996). The shift of the Q_y transition energies of both Bpheos is linear (and similar) over the whole pressure range of the experiment, suggesting that the compressibility of the RC structure around these cofactors remains constant from atmospheric pressure to ~0.6 GPa.

As it was already pointed out, the behavior of the Q_y absorption band of the primary electron donor under pressure is much more intricate (Figs. 3 and 4). At low pressures (from atmospheric pressure to 0.2 GPa), it experiences a redshift ~1.7-fold larger than the Q_y transitions of the accessory Bchl. Hydrogen bonds between the acetyl carbonyls of Bchls (either monomer or within a special pair dimer) and the surrounding protein residues have been well documented experimentally (Sturgis et al., 1997, 1995a,b; Olsen et al., 1994, 1997; Fowler et al., 1994). It was, in particular, shown that there is a strong correlation between the redshift of the Q_y electronic transition energy of Bchl and the downshift of the stretching mode vibrational frequency of its acetyl carbonyl, induced by the formation of the H-bond (Sturgis et al., 1998). This phenomenon was also observed in RCs of *Rb. sphaeroides* in which a tyrosine had been introduced to form a H-bond with the P_M molecule of the primary electron donor (Ivancich et al., 1998). In this work, between 1 atm and 0.2 GPa, a 5-cm^{-1} downshift of the stretching mode of the acetyl carbonyl from P_L, from 1620 to 1615 cm^{-1}, has been observed. According to Sturgis and Robert (1997), such a downshift would correspond, in light-harvesting proteins, to a 50-cm^{-1} redshift in the Bchl Q_y transition energy. This mechanism could thus provide a simple explanation for about half of the downshift experienced by the Q_y of P between 0.0001 and 0.2 GPa, as due to the increase in the strength of the H-bond between His_{L168} and P_L. As discussed above, the conformation of both Bchl molecules constituting P also changes in this pressure range. Such a conformational change together with the expected increase of the intermolecular electronic coupling between the P_L and P_M dimer molecules may constitute the major part of the rest of the observed downshift of the Q_y transition energy of P in this low pressure range.

At intermediate pressures, 0.2–0.3 GPa, the position of the Q_y absorption band of P remains nearly the same. It is of note that this pressure range corresponds to that at which, in FT-Raman experiments the P protein binding site stops reorganizing measurably according to pressure. This does not mean, however, that the changes observed between atmospheric pressure and 0.2 GPa may formally be attributed to the observed reorganizations in this pressure range. At pressures above 0.3 GPa, the position of the Q_y of P starts to redshift according to pressure with an even larger rate than at low pressures. Notably, the redshift of the P band at high pressures is accompanied by a rather dramatic drop of the integrated area of the band. In the absence of significant local structural reorganization of the pigment binding site, which is confirmed by the FT Raman data, it is likely that the change of the absorption spectrum of P arises

from a pressure-induced perturbation of the electronic states of the dimer. Indeed, as the P_L and P_M molecules are in van der Waals contact, even very slight changes in their relative spatial structure may induce drastic changes of the P electronic structure, which could induce important variations of the relative intensities of the different P transitions (Warshel et al., 1994; Warshel and Parson, 1987; Parson and Warshel, 1987; Parson et al., 1990). At the pressures where this phenomenon occurs (0.2 GPa and above), the evolution with time of the absorption spectra of the RC (Fig. 5) reveals that their structure requires hours to reach quasi-equilibrium. This may be in part due to the increase in viscosity of the medium upon pressure increase.

Finally, an interesting feature of this particular RC protein is the absence of the carotenoid cofactor. In the wild-type protein this chromophore is located close to the macrocycle of the accessory bacteriochlorophyll B_M and has contacts with the bacteriopheophytin on the M-branch. In general, there are few differences between the x-ray crystal structures of the wild type (namely, carotenoid-containing) and carotenoid-free RC proteins. It is possible that the presence in the protein of an internal space, induced by the absence of this molecule, would increase the local compressibility around the carotenoid binding site and would thus influence the stability of neighboring sub-structures. Comparative pressure studies of wild-type and carotenoid-free RCs are currently underway in our laboratory to clear up this last point.

REFERENCES

Benson, A. M., and H. G. Dricamer. 1957. Stretching vibrations in condensed systems. *J. Chem. Phys.* 27:1164–1174.

Böse, S. K. 1963. Media for anaerobic growth of photosynthetic bacteria. *In* Bacterial Photosynthesis. H. Gest, A. Pietro, and L. P. Vermon, editors. The Antioch Press, Yellow Springs, OH. 501–510.

Clayton, R. K., and R. T. Wang. 1971. Photochemical reaction centers from *Rhodopseudomonas spheroides*. *Methods Enzymol.* 23:696–704.

Cogdell, R. J., and H. A. Frank. 1987. How carotenoids function in photosynthetic bacteria. *Biochim. Biophys. Acta.* 895:63–79.

Deisenhofer, J., O. Epp, K. Miki, R. Huber, and H. Michel. 1984. X-ray structure analysis of a membrane protein complex. Electron density map at 3 Å resolution and a model of the chromophores of the photosynthetic reaction center from *Rhodopseudomonas viridis*. *J. Mol. Biol.* 180:385–398.

Deisenhofer, J., and H. Michel. 1989. The photosynthetic reaction center from the purple bacterium *Rhodopseudomonas viridis*. *Chem. Scr.* 29:205–220, 4 plates.

Feher, G. 1971. Some chemical and physical properties of a bacterial reaction center particle and its primary photo-chemical reactants. *Photochem. Photobiol.* 14:373–387.

Feher, G., J. P. Allen, M. Y. Okamura, and D. C. Rees. 1989. Structure and function of bacterial photosynthetic reaction centers. *Nature.* 339:111–116.

Fisher, H., and H. Orth. 1937. Die Chemie des Pyrrols. Vol. 2, part 1. Akad. Verlagsges, Leipzig, Germany.

Fisher, H., and A. Stern. 1940. Die Chemie des Pyrrols. Vol. 2, part 2. Akad. Verlagsges, Leipzig, Germany.

Fowler, G. J. S., G. D. Sockalingum, B. Robert, and C. N. Hunter. 1994. Blue shifts in bacteriochlorophyll absorbance correlate with changed hydrogen bonding patterns in light-harvesting 2 mutants of *Rhodobacter sphaeroides* with alterations at alpha-Tyr-44 and alpha-Tyr-45. *Biochem. J.* 299:695–700.

Frank, H. A., and R. J. Cogdell. 1996. Carotenoids in photosynthesis. *Photochem. Photobiol.* 63:257–264.

Freiberg, A., A. Ellervee, P. Kukk, A. Laisaar, M. Tars, and K. Timpmann. 1993. Pressure effects on spectra of photosynthetic light-harvesting pigment-protein complexes. *Chem. Phys. Lett.* 214:10–16.

Fyfe, P. K., K. E. McAuley-Hecht, J. P. Ridge, S. M. Prince, G. Fritzsch, N. W. Isaacs, R. J. Cogdell, and M. R. Jones. 1998. Crystallographic studies of mutant reaction centers from *Rhodobacter sphaeroides*. *Photosynth. Res.* 55:133–140.

Hoganson, C. W., M. W. Windsor, D. I. Farkas, and W. W. Parson. 1987. Pressure effects on the photochemistry of bacterial photosynthetic reaction centers from *Rhodobacter sphaeroides* R-26 and *Rhodopseudomonas viridis*. *Biochim. Biophys. Acta.* 892:275–283.

Ivancich, A., K. Artz, J. C. Williams, J. P. Allen, and T. A. Mattioli. 1998. Effects of hydrogen bonds on the redox potential and electronic structure of the bacterial primary electron donor. *Biochemistry.* 37:11812–11820.

Ivancich, A., M. Lutz, and T. A. Mattioli. 1997. Temperature-dependent behavior of bacteriochlorophyll and bacteriopheophytin in the photosynthetic reaction center from *Rhodobacter sphaeroides*. *Biochemistry.* 36:3242–3253.

Laird, B. B., and J. L. Skinner. 1989. Microscopic theory of reversible pressure broadening in hole-burning spectra of impurities in glasses. *J. Chem. Phys.* 90:3274–3281.

Lapouge, K., A. Näveke, A. Gall, J. Seguin, H. Scheer, J. Sturgis, and B. Robert. 1999. Conformation of bacteriochlorophyll molecules in photosynthetic proteins from purple bacteria. *Biochemistry.* 38:11115–11121.

Lapouge, K., A. Näveke, J. N. Sturgis, G. Hartwich, D. Renaud, I. Simonin, M. Lutz, H. Scheer, and B. Robert. 1998. Non-bonding molecular factors influencing the stretching wavenumbers of the conjugated carbonyl groups of bacteriochlorophyll *a*. *J. Raman Spectrosc.* 29:977–981.

Mattioli, T. A., A. Hoffmann, B. Robert, B. Schrader, and M. Lutz. 1991a. Near-IR FT resonance Raman spectroscopy of the primary donor in bacterial reaction center proteins. *Spec. Publ. R. Soc. Chem.* 94:47–50.

Mattioli, T. A., A. Hoffmann, B. Robert, B. Schrader, and M. Lutz. 1991b. Primary donor structure and interactions in bacterial reaction centers from near-infrared Fourier transform resonance Raman spectroscopy. *Biochemistry.* 30:4648–4654.

Mattioli, T. A., A. Hoffmann, D. G. Sockalingum, B. Schrader, B. Robert, and M. Lutz. 1993. Application of near-IR Fourier transform resonance Raman spectroscopy to the study of photosynthetic proteins. *Spectrochim. Acta A.* 49A:785–799.

Mattioli, T. A., J. C. Williams, J. P. Allen, and B. Robert. 1994. Changes in primary donor hydrogen-bonding interactions in mutant reaction centers from *Rhodobacter sphaeroides*: identification of the vibrational frequencies of all the conjugated carbonyl groups. *Biochemistry.* 33:1636–1643.

McAuley-Hecht, K. E., P. K. Fyfe, J. P. Ridge, S. M. Prince, C. N. Hunter, N. W. Isaacs, R. J. Cogdell, and M. R. Jones. 1998. Structural studies of wild-type and mutant reaction centers from an antenna-deficient strain of *Rhodobacter sphaeroides*: monitoring the optical properties of the complex from bacterial cell to crystal. *Biochemistry.* 37:4740–4750.

Michel, H., and J. Deisenhofer. 1988. Structure and function of the photosynthetic reaction center from *Rhodopseudomonas viridis*. *Pure Appl. Chem.* 60:953–558.

Mozhaev, V. V., K. Heremans, J. Frank, P. Masson, and C. Balny. 1996. High pressure effects on protein structure and function. *Proteins.* 24:81–91.

Näveke, A., K. Lapouge, J. N. Sturgis, G. Hartwich, I. Simonin, H. Scheer, and B. Robert. 1997. Resonance Raman spectroscopy of metal-substituted bacteriochlorophylls: characterization of Raman bands sensitive to bacteriochlorin conformation. *J. Raman Spectrosc.* 28: 599–604.

Olsen, J. D., G. D. Sockalingum, B. Robert, and C. N. Hunter. 1994. Modification of a hydrogen bond to a bacteriochlorophyll a molecule in the light-harvesting 1 antenna of *Rhodobacter sphaeroides*. *Proc. Natl. Acad. Sci. U.S.A.* 91:7124–7128.

Olsen, J. D., J. N. Sturgis, W. H. J. Westerhuis, G. J. S. Fowler, C. N. Hunter, and B. Robert. 1997. Site-directed modification of the ligands to the bacteriochlorophylls of the light-harvesting LH1 and LH2 complexes of *Rhodobacter sphaeroides*. *Biochemistry.* 36:12625–12632.

Parson, W. W., Z. T. Chu, and A. Warshel. 1990. Electrostatic control of charge separation in bacterial photosynthesis. *Biochim. Biophys. Acta.* 1017:251–272.

Parson, W. W., and R. J. Cogdell. 1975. Primary photochemical reaction of bacterial photosynthesis. *Biochim. Biophys. Acta.* 416:105–149.

Parson, W. W., and A. Warshel. 1987. Spectroscopic properties of photosynthetic reaction centers. II. Application of the theory to *Rhodopseudomonas viridis*. *J. Am. Chem. Soc.* 109:6152–6163.

Pieper, J., K. D. Irrgang, M. Ratsep, J. Voigt, G. Renger, and G. J. Small. 2000. Assignment of the lowest Qy-state and spectral dynamics of the CP29 chlorophyll a/b antenna complex of green plants: a hole-burning study. *Photochem. Photobiol.* 71:574–581.

Pieper, J., M. Raetsep, R. Jankowiak, K.-D. Irrgang, J. Voigt, G. Renger, and G. J. Small. 1999. Qy-level structure and dynamics of solubilized light-harvesting complex II of green plants: pressure and hole burning studies. *J. Phys. Chem. A.* 103:2412–2421.

Raetsep, M., T. W. Johnson, P. R. Chitnis, and G. J. Small. 2000. The red-absorbing chlorophyll a antenna states of photosystem I: a hole-burning study of *Synechocystis* sp. PCC 6803 and its mutants. *J. Phys. Chem. B.* 104:836–847.

Reddy, N. R. S., R. J. Cogdell, L. Zhao, and G. J. Small. 1993. Nonphotochemical hole burning of the B800–B850 antenna complex of *Rhodopseudomonas acidophila*. *Photochem. Photobiol.* 57:35–39.

Reddy, N. R. S., R. Jankowiak, and G. J. Small. 1995. High-pressure hole-burning studies of the bacterio[chloro]phyll a antenna complex from *Chlorobium tepidum*. *J. Phys. Chem.* 99:16168–16178.

Reddy, N. R. S., and G. J. Small. 1996. Spectral hole burning: methods and applications to photosynthesis. *Adv. Photosynth.* 3:123–136.

Reddy, N. R. S., H.-M. Wu, R. Jankowiak, R. Picorel, R. J. Cogdell, and G. J. Small. 1996. High pressure studies of energy transfer and strongly coupled bacteriochlorophyll dimers in photosynthetic protein complexes. *Photosynth. Res.* 48:277–289.

Redline, N. L., M. W. Windsor, and R. Menzel. 1991. The effect of pressure on the secondary (200 ps) charge transfer step in bacterial reaction centers of *Rhodobacter sphaeroides* R-26. *Chem. Phys. Lett.* 186:204–209.

Robert, B. 1996. Resonance Raman studies in photosynthesis: chlorophyll and carotenoid molecules. *In* Biophysical Techniques in Photosynthesis. A. Amez and A. Hoff, editors. Kluwer Academic Publishers, Amsterdam. 161–276.

Roy, C., D. Lancaster, U. Ermler, and H. Michel. 1995:The structures of photosynthetic reaction centers from purple bacteria as revealed by x-ray crystallography. *In* Anoxygenic Photosynthetic Bacteria. R. E. Blakenship, M. T. Madigan, and C. E. Bauer, editors. Kluwer Academic Publishers, Dordrecht, The Netherlands. 503–526.

Schägger, H., and G. von Jagow. 1987. Tricine-sodium dodecyl sulfate-polyacrylamide gel electrophoresis for the separation of proteins in a range from 1 to 100 kDa. *Anal. Biochem.* 166:368–379.

Sesselmann, T., W. Richter, D. Haarer, and H. Morawitz. 1987. Spectroscopic studies of impurity-host interactions in dye-doped polymers: hydrostatic-pressure effects versus temperature effects. *Phys. Rev. B.* 36:7601–77611.

Small, G. J. 1995. On the validity of the standard model for primary charge separation in the bacterial reaction center. *Chem. Phys.* 197:239–257.

Stowell, M. H. B., T. M. McPhillips, D. C. Rees, S. M. Solitis, E. Abresch, and G. Feher. 1997. Light-induced structural changes in photosynthetic reaction center: implications for mechanism of electron-proton transfer. *Science.* 276:812–816.

Sturgis, J. N., A. Gall, A. Ellervee, A. Freiberg, and B. Robert. 1998. The effect of pressure on the bacteriochlorophyll a binding sites of the core antenna complex from *Rhodospirillum rubrum*. *Biochemistry.* 37: 14875–14880.

Sturgis, J. N., G. Hageman, M. H. Tadros, and B. Robert. 1995a. Biochemical and spectroscopic characterization of the B800–850 light-harvesting complex from *Rhodobacter sulfidophilus* and its B800–830 spectral form. *Biochemistry.* 34:10519–10524.

Sturgis, J. N., V. Jirsakova, F. Reiss-Husson, R. J. Cogdell, and B. Robert. 1995b. Structure and properties of the bacteriochlorophyll binding site in peripheral light-harvesting complexes of purple bacteria. *Biochemistry.* 34:517–523.

Sturgis, J. N., J. D. Olsen, B. Robert, and C. N. Hunter. 1997. Functions of conserved tryptophan residues of the core light-harvesting complex of *Rhodobacter sphaeroides*. *Biochemistry.* 36:2772–2778.

Sturgis, J. N., and B. Robert. 1997. Pigment binding site and electronic properties in light-harvesting proteins of purple bacteria. *J. Phys. Chem. B.* 101:7227–7231.

Tars, M., A. Ellervee, P. Kukk, A. Laisaar, A. Saarnak, and A. Freiberg. 1994. Photosynthetic proteins under high pressure. *Lietuvos Fizikos Žurnalas.* 34:320–328.

Tars, M., A. Ellervee, M. R. Wasielewski, and A. Freiberg. 1998. Biomolecular electron transfer under high hydrostatic pressure. *Spectrochim. Acta A.* 54A:1177–1189.

Van Grondelle, R. 1985. Excitation energy transfer, trapping and annihilation in photosynthetic systems. *Biochim. Biophys. Acta.* 811:147–195.

Wachtveitl, J., J. W. Farchaus, R. Das, M. Lutz, B. Robert, and T. A. Mattioli. 1993. Structure, spectroscopic, and redox properties of *Rhodobacter sphaeroides* reaction centers bearing point mutations near the primary electron donor. *Biochemistry.* 32:12875–12886.

Warshel, A., Z. T. Chu, and W. W. Parson. 1994. On the energetics of the primary electron-transfer process in bacterial reaction centers. *J. Photochem. Photobiol. A.* 82:123–128.

Warshel, A., and W. W. Parson. 1987. Spectroscopic properties of photosynthetic reaction centers. I. Theory. *J. Am. Chem. Soc.* 109:6143–6152.

Windsor, M. W., and R. Menzel. 1989. Effect of pressure on the 12 ns charge recombination step in reduced bacterial reaction centers of *Rhodobacter sphaeroides* R-26. *Chem. Phys. Lett.* 164:143–150.

Wu, H.-M., M. Ratsep, R. Jankowiak, R. J. Cogdell, and G. J. Small. 1997a. Comparison of the LH2 antenna complexes of *Rhodopseudomonas acidophila* (strain 10050) and *Rhodobacter sphaeroides* by high-pressure absorption, high-pressure hole burning, and temperature-dependent absorption spectroscopies. *J. Phys. Chem. B.* 101:7641–7653.

Wu, H.-M., M. Ratsep, R. Jankowiak, R. J. Cogdell, and G. J. Small. 1998. Hole-burning and absorption studies of the LH1 antenna complex of purple bacteria: effects of pressure and temperature. *J. Phys. Chem. B.* 102:4023–4034.

Wu, H.-M., M. Ratsep, I.-J. Lee, R. J. Cogdell, and G. J. Small. 1997b. Exciton level structure and energy disorder of the B850 ring of the LH2 antenna complex. *J. Phys. Chem. B.* 101:7654–7663.

Wu, H., M. Ratsep, C. S. Young, R. Jankowiak, R. E. Blankenship, and G. J. Small. 2000. High-pressure and stark hole-burning studies of chlorosome antennas from *Chlorobium tepidum*. *Biophys. J.* 79: 1561–1572.

Wu, H.-M., S. Savikhin, N. R. S. Reddy, R. Jankowiak, R. J. Cogdell, W. S. Struve, and G. J. Small. 1996. Femtosecond and hole-burning studies of B800's excitation energy relaxation dynamics in the LH2 antenna complex of *Rhodopseudomonas acidophila* (strain 10050). *J. Phys. Chem.* 100:12022–12033.

Yeates, T. O., H. Komiya, A. Chirino, D. C. Rees, J. P. Allen, and G. Feher. 1988. Structure of the reaction center from *Rhodobacter sphaeroides* R-26 and 2.4.1. IV. Protein-cofactor (bacteriochlorophyll, bacteriopheophytin, and carotenoid) interactions. *Proc. Natl. Acad. Sci. U.S.A.* 85:7993–7997.

Zhou, Y., S. A. Lee, and A. Anderson. 1996. Raman studies of molecular crystals at high pressures. III. Methylene iodide. *J. Raman Spectrosc.* 27:499–502.